Archives of Materials Science and Engineering

Volume 35
Issue 2
February 2009
Pages 83-90

International Scientific Journal
published monthly by the
World Academy of Materials
and Manufacturing Engineering

The investigations of hot-deformability and structure of high-temperature Fe–Ni alloy

K.J. Ducki*, D. Kuc
Materials Science Department, Silesian University of Technology,
ul. Krasińskiego 8, 40-019 Katowice, Poland
* Corresponding author: E-mail address: kazimierz.ducki@polsl.pl

Received 12.02.2007; published in revised form 01.02.2009

ABSTRACT

Purpose: This study describes the influence of initial austenite grain size and parameters of hot plastic deformation on the deformability and structure of high-temperature Fe–Ni austenitic alloy of A-286 type.

Design/methodology/approach: The hot deformation characteristics of the alloy were investigated by hot torsion tests using torsion plastometer. The tests were executed at constant strain rates of 0.1 and 1.0 s^{-1}, at a testing temperature in the range from 900 to 1150°C. The structural inspections were performed on microsections taken from plastometric samples after so called "freezing".

Findings: Plastic properties of the alloy were characterized by the worked out flow curves and the temperature relationships of flow stress and the strain limit. The relationship between the peak stress (σ_{pp}) and the Zoner-Hollomon parameter (Z) were described by power function. Activation energy for hot working (Q) was assessed for the alloy after two variants of previous heating. The examinations performed, focusing on the influence of hot working parameters on the structure of austenitic alloy, revealed subsequently occurring processes of dynamic recovery, recrystallization and repolygonization.

Practical implications: Characteristics of the alloy plastic properties during hot deformation depend considerably on the initial soaking temperature and hot deformation parameters. Optimum values of yield stress and strain limit were obtained for the alloy after its initial soaking at 1100°C/2h and strain rate of 0.1 s^{-1} in the temperature range of 1050-950°C.

Originality/value: An increase of the alloy deformation temperature led to a growth of the size of subgrains with a simultaneous decrease of their internal dislocation density. The influence of the strain rate of the alloy on the size of subgrains and dislocation density is complex by nature and depends on the initial size of the austenite grains and on the mechanism of the dynamic recrystallization process.

Keywords: Metallic alloys; Hot deformation; Recrystallization; TEM

Reference to this paper should be given in the following way:

K.J. Ducki, D. Kuc, The investigations of hot-deformability and structure of high-temperature Fe–Ni alloy, Archives of Materials Science and Engineering 35/2 (2009) 83-90.

MATERIALS

1. Introduction

The behaviour of metals and alloys during hot plastic deformation has a complex nature and it varies with the changing of such process parameters as [1, 3, 5, 8, 11, 15]: deformation size, strain rate and temperature. The high-temperature plastic deformation is coupled with dynamic processes of recovery influencing the structure and properties of alloys. One of crucial issues is finding the interdependence between the hot plastic deformation process parameters, the structure and properties. Since the sixties of the last century, theoretical and experimental

investigations have been carried out to find those interdependencies for steels and alloys.

In the recent years, the constitutive equations describing hot plastic deformation processes have started to take into account the so-called internal variables determining the material condition. These variables include substructural parameters such as [10, 13, 14, 16]: dislocation density, subgrain size, subgrain misorientation angle, recrystalized volume fraction and stacking fault energy (SFE). Determination of the above-mentioned parameters of a deformed material structure description requires the application of analytical methods primarily based on transmission electron microscopy (TEM). Taking those substructure parameters into consideration in calculations should enable the correct modelling of structural phenomena during hot plastic deformation and enhance the technological processes control for the purpose of obtaining the assumed structures of required properties.

In the present study, investigations were undertaken of the influence of the austenite initial structure and the hot plastic forming parameters on the deformability, subgrain size and dislocation density in a high-temperature creep resisting Fe–Ni austenitic alloy of the A-286 type.

2. Material and procedure

Investigations of the alloy deformability were performed by the hot torsion method in a 7 MNG torsion plastometer manufactured by Setaram. Plastometric tests were carried out every 50°C at a temperature range of 900-1150°C, with applying constant soaking time of 10 minutes at the given temperature. Solid cylindrical samples (ϕ 6,0×50 mm) were twisted at a rotational speed of 50 and 500 rpm, which corresponds to the deformation rate of 0.1 and 1.0 s^{-1}. After deformation until failure, the samples were cooled with water by direct introduction of the liquid into the furnace heating chamber.

The investigations were carried out on rolled bars, 16 mm in diameter made of Fe–Ni austenitic alloy (marked X5NiCrTi25-15) of the A-286 type. The chemical composition is given in Table 1. In order to model the conditions of alloy heating prior to plastic processing, the investigations were carried out on samples after initial soaking at high temperatures. Sections of rolled bars, which the samples for investigations were made of, were subjected to two variants of preheating, i.e. 1100°C/2h and 1150°C/2h with subsequent cooling in water. Thermal processing of this type corresponds to the soaking parameters of the analysed alloy prior to hot plastic processing [7].

The data obtained in the plastometric torsion test were entered in an Excel spreadsheet in the form of columns containing the recorded values. Processing of the measured data by means of filtration, cutting, shrinking and planishing was conducted using the Matlab 6 program. A correction of the torque moment, due to diversified rotational speed values and increase of the sample temperature during torsion, was calculated by the method of joint action of speed and temperature from the following relations [4, 12]:

$$M''' = M + \Delta M''' \tag{1}$$

$$\Delta M''' = M(N, \dot{N}, T) - M(N, \dot{N}_r, T + \Delta T) \tag{2}$$

$$\Delta M''' = A \cdot N^B \cdot \exp(C \cdot N) \cdot \dot{N}^{D+\frac{E}{T}} \cdot \exp\left(\frac{F}{T}\right) + \tag{3}$$

$$- A \cdot N^B \exp(C \cdot N) \cdot \dot{N}^{D+\frac{E}{T+\Delta T}} \cdot \exp\left(\frac{F}{T+\Delta T}\right)$$

where:

- M – recorded torque moment, [Nm;];
- M''' – corrected torque moment value, [Nm;];
- ΔM – torque moment correction taking account of a joint action of speed and temperature, [Nm];
- N – number of sample torsions;
- $\dot{N}$ – given torsion speed [rpm];
- $\dot{N}_r$ – recorded rotational speed [rpm];
- T – deformation temperature, [°C];
- ΔT – temperature increment during torsion, [°C];

A, B, C, D, E, E , F – material constants.

The corrected data constituted a basis for the determination of equivalent deformation (ε) as a function of the number of the sample's rotations during torsion (Hadasik, 2005; Schindler and Boruta, 1998):

$$\varepsilon = \frac{2}{\sqrt{3}} \times \operatorname{arcsinh}\left(\frac{\pi \bar{R} N}{L}\right) \tag{4}$$

where:

- $\bar{R}$ – equivalent radius corresponding to 2/3 of the external radius of sample R;
- L – measured length of the sample.

Yield stress (σ_p) was determined according to relation (5) taking account of the corrected torque moment (M'''), sample radius (R), parameters (m, p) and axial force (F_o) [4, 12]:

$$\sigma_p = \left[\left(\frac{\sqrt{3} \cdot M'''}{2\pi R^3}\right)^2 \times (3 + p + m)^2 + \left(\frac{F_o}{\pi R^2}\right)\right]^{0,5} \tag{5}$$

where:

p – parameter reflecting stress sensitivity to deformation size;
m – parameter reflecting stress sensitivity to deformation rate.

On the flow curves determined, the following parameters characterising plastic properties of the alloy in the torsion test were defined:

- σ_{pp} – maximum yield stress on the flow curve;
- ε_p – deformation corresponding to the maximum yield stress;
- σ_f stress at which the sample is subject to failure;
- ε_f deformation at which the sample is subject to failure, the so-called threshold deformation.

Table 1.
Chemical composition of the investigated Fe–Ni austenitic alloy

Content of an element, wt.%														
C	Si	Mn	P	S	Cr	Ni	Mo	V	W	Ti	Al	Co	B	N
0.05	0.55	1.25	0.026	0.016	14.3	24.5	1.34	0.41	0.10	1.88	0.16	0.08	0.007	0.0062

Relations between the yield stress, the alloy deformation and the deformation conditions were described using the Zener-Hollomon's parameter (Z) [4, 12]:

$$Z = \dot{\varepsilon} \times \exp\left(\frac{Q}{RT}\right) = A \times \left[\sinh\left(\alpha\sigma_{pp}\right)\right]^n \quad (6)$$

where:

$\dot{\varepsilon}$ – deformation rate; T – deformation temperature; R – gas constant;

Q – activation energy of the plastic deformation process.

The activation energy of the hot plastic deformation process (Q) was determined in accordance with the procedure specified in the work by Schindler and Boruta [12]. The solution algorithm consisted in transforming equation (6) to the following form:

$$\dot{\varepsilon} = A \times \exp\left(\frac{-Q}{RT}\right)\left[\sinh(\alpha\sigma_{pp})\right]^n \quad (7)$$

Further procedure was based on solving equation (7) by a graphic method with the application of a regression analysis.

Structural examinations were carried out by applying the thin film technique, using a JEM-100B Joel's transmission electron microscope at the accelerating voltage of 100 kV. The material was cut into thin films of ca. 1 mm thickness by means of spark erosion cutting from a distance of ca. 2/3 of the sample radius, in parallel to its axis. Initial thinning of the samples to a thickness of ca. 0.08-0.03 mm was carried out using mechanical grinding machines. Next, using a matrix, disks of a diameter of 3 mm were cut out. The obtained disks were thinned out by a two-sided stream electropolishing method in a Tenupol device manufactured by Struers. A brand A-8 agent was used for iron alloys (950 ml. acetic acid CH_3COOH, 50 ml. perchloric acid $HClO_4$), cooled to a temperature of 11°C with polishing voltage of 65 V. On the basis of direct measurements conducted on photographs from an electron microscope, the mean area of subgrain as well as mean dislocation density were determined for the samples analysed.

The mean area of a subgrain plane section ($\bar{A}$) was determined using the planimetric method in a semi-automatic picture analyser, MOP AMO 3. The measurements were carried out on photographs from a transmission microscope in a 1:1 scale. The analysed microareas of the thin films enabled the measuring of ca. 150 subgrains for each sample.

The mean dislocation density was calculated by a method consisting in counting the points of intersection of a grid superimposed on the microscope photograph with the dislocation lines. Dislocation density (ρ) was determined on thin films according to the relation provided by Klaar *et al*. [6] and Martin *et al*. [9]:

$$\rho = \frac{x \cdot (n_1 / l_1 + n_2 / l_2)}{t} \quad [m^{-2}] \quad (8)$$

where:

x – fraction of invisible dislocations with a Burgers vectors a/2 < 111> for the A1 lattice;

$l_{1\,(2)}$ – total length of the horizontal (vertical) lattice lines;

$n_{1(2)}$ – number of intersections of the horizontal (vertical) lattice lines with dislocations;

t – thickness of foil.

Thickness of the thin foil (t) at the analysed locations was determined by an extinction contours method characterised by a high measurement accuracy within the limits of ±5 to ±8%.

3. Results of the alloy deformability

The results of the plastometric investigations in the form of the calculated alloy torsion curves for two options of initial soaking are presented in Figs. 1-4. The curves obtained for the option of initial soaking at 1100°C/2h and torsion speed amounting to 0.1 s^{-1}, display a shape characteristic of a material in which recovery and dynamic recrystallization processes take place (Fig. 1). High deformation values were obtained for the alloy in a wide range of torsion temperatures, i.e. 950-1100°C. An increase of torsion speed to 1.0 s^{-1} results in a significant increase of yield stress values and a distinct decrease of the alloy deformability at all temperatures analysed (Fig. 2). This phenomenon can be explained by a higher speed of the alloy strengthening and too slow removal of the reinforcement as a result of recovery and dynamic recrystallization.

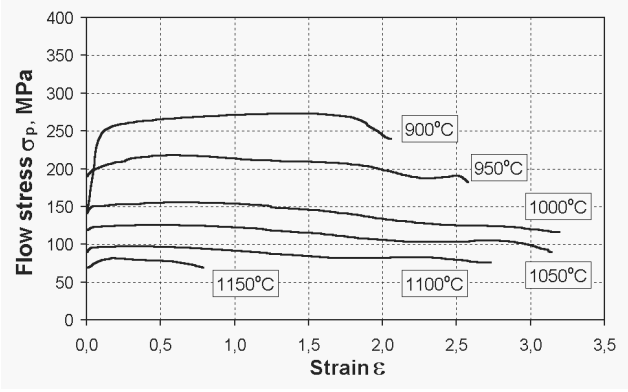

Fig. 1. Influence of deformation temperature on the form of alloy flow curves after pre-soaking at 1100°C/2h; strain rate 0.1s^{-1}

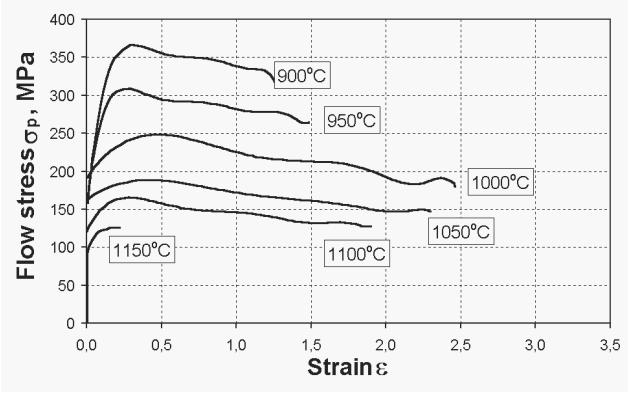

Fig. 2. Influence of deformation temperature on the form of alloy flow curves after pre-soaking at 1100°C/2h; strain rate 1.0 s^{-1}

An increase of the initial soaking temperature to 1150°C/2h significantly reduces the alloy deformability for the two torsion speeds, both at low and high deformation temperatures (Figs. 3 and 4). In this case, fairly high deformation values were obtained for the alloy in a narrow range of torsion temperatures, i.e. 1000-1050°C. Such behaviour of the alloy may be explained by a larger

growth of austenite subgrain at this soaking temperature and, consequently, lower recovery and dynamic recrystallization rates.

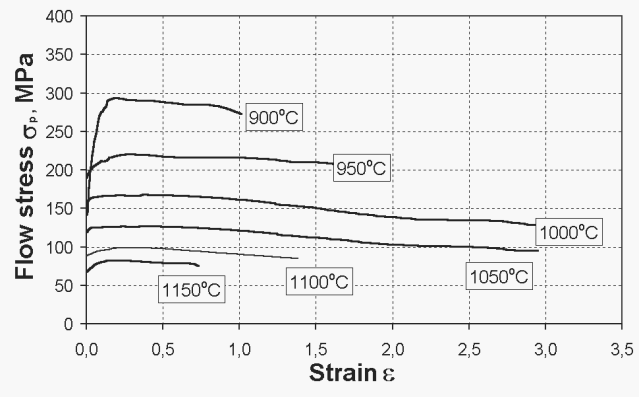

Fig. 3. Influence of deformation temperature on the form of alloy flow curves after pre-soaking at 1150°C/2 h; strain rate 0.1 s^{-1}

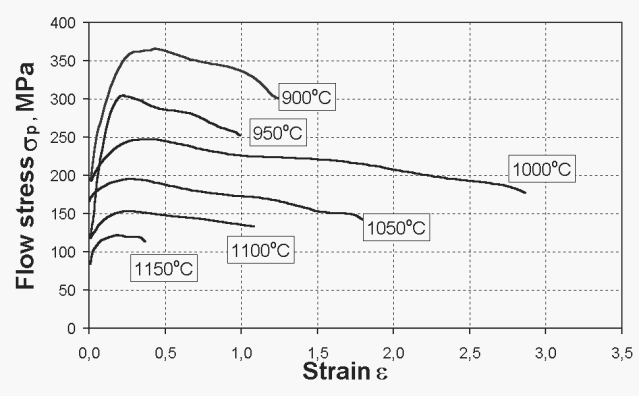

Fig. 4. Influence of deformation temperature on the form of alloy flow curves after pre-soaking at 1150°C/2 h; strain rate 1.0 s^{-1}

The values determined for the maximum yield stress (σ_{pp}), maximum deformation (ε_p), stress until failure (σ_f) and threshold deformation (ε_f) depending on the temperature and speed of alloy torsion are provided in Table 2. For the option of initial soaking at 1100°C/2h and torsion speed of 0.1s^{-1}, the alloy under discussion shows a contiuous drop of σ_{pp} and σ_f from values 277 and 240 MPa at a temperature of 900°C to the value of 81 and 70 MPa at 1150°C. The threshold deformation (ε_f) rises initially together with the torsion temperature, reaching the maximum of (3.19/3.14) at 1000-1050°C, and then falls. An increase of the torsion speed to 1.0 s^{-1} results in an increase of σ_{pp} and σ_f to maximum values of 367 and 315 MPa at the temperature of 900°C and a decrease of the threshold deformation to the maximum of 2.47/2.34 at 1000-1050°C.

An increase of the alloy initial soaking temperature to 1150°C/2h at a torsion speed of 1s^{-1} results in a slight increase of σ_{pp} and σ_f to maximum values of 367 and 272 MPa at 900°C, and decrease of ε_f to the maximum of 2.92 in the range of 1000÷1050°C. An increase of the torsion speed to 1.0 s^{-1} results in further increase of the σ_{pp} and σ_f values to maximum values of 370 and 300 MPa at 900°C, and decrease of ε_f to the maximum values of 2.89/1.75 at the temperature of 1000-1050°C.

The dependencies between yield stress (σ_{pp}) and Zener-Hollomon's parameter are presented in Figs. 5 and 6. For both options of initial soaking, a power dependence (R^2 = 0,92-0,93) of the alloy yield stress was obtained as a function of the Z parameter. So determined function dependencies between the maximum yield stress (σ_{pp}) and the (Z) parameter had a form of power function:

– for the alloy after initial soaking at 1100°C/2h:

$$\sigma_{pp} = 0{,}52 \times Z^{0{,}13} \quad (9)$$

– for the alloy after initial soaking at 1150°C/2h:

$$\sigma pp = 0{,}37 \times Z0{,}12 \quad (10)$$

Higher values of the Z parameter for the alloy after initial soaking at1150°C/2h result from higher values of the plastic deformation activation energy. For the alloy after initial soaking at 1100°C/2h, the activation energy estimated in the range of the deformation temperatures applied (900-1150°C) amounted to Q = 483 kJ/mol. In the case of deformation of the alloy after initial soaking at1150°C/2h, the activation energy was higher and its value amounted to Q = 563 kJ/mol.

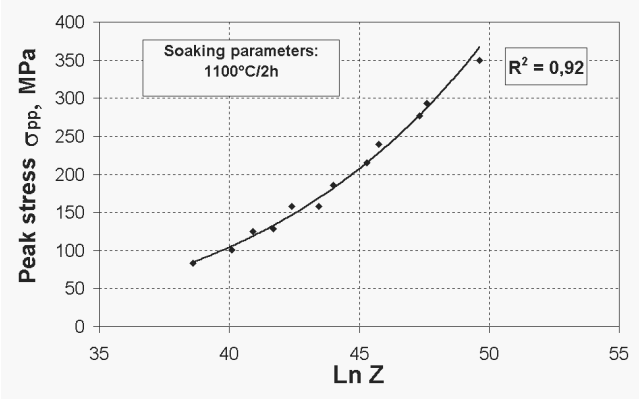

Fig. 5. Relation between maximum flow stress of alloy an Zener-Hollomon parameter; pre-soaking of the alloy: 1100°C/ 2h

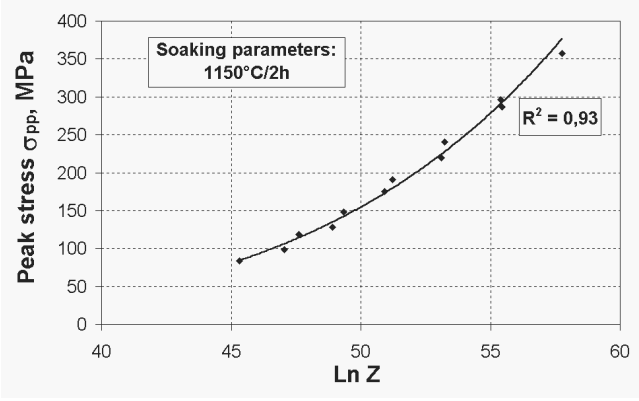

Fig. 6. Relation between maximum flow stress of alloy an Zener-Hollomon parameter; pre-soaking of the alloy: 1150°C/ 2h

Table 2.
The indexes of the Fe–Ni alloy plastic properties determine from flow curves

Pre-soaking parameters	Deformation parameters		The indexes of alloy plastic properties			
	Temperature,°C	Strain rate, s^{-1}	σ_{pp}, MPa	ε_p	σ_f, MPa	ε_f
1100°C/2h	900	0.1	277	1.52	240	2.05
	950	0.1	215	0.66	183	2.57
	1000	0.1	158	0.53	117	3.19
	1050	0.1	128	0.59	90	3.14
	1100	0.1	97	0.27	76	2.73
	1150	0.1	81	0.18	70	0.78
	900	1.0	367	0.32	315	1.26
	950	1.0	305	0.26	265	1.45
	1000	1.0	248	0.49	180	2.47
	1050	1.0	189	0.42	147	2.34
	1100	1.0	165	0.28	128	1.93
	1150	1.0	125	0.18	126	0.36
1150°C/2h	900	0.1	367	0.18	272	1.06
	950	0.1	220	0.28	207	1.62
	1000	0.1	166	0.26	188	2.92
	1050	0.1	124	0.21	95	2.92
	1100	0.1	99	0.20	84	1.40
	1150	0.1	82	0.16	75	0.72
	900	1.0	370	0.39	300	1.24
	950	1.0	306	0.22	252	0.99
	1000	1.0	247	0.36	177	2.89
	1050	1.0	194	0.32	142	1.75
	1100	1.0	151	0.27	133	1.08
	1150	1.0	122	0.20	113	0.36

4. Results of the alloy structure

After initial soaking at 1100°C/2h, the analysed Fe–Ni alloy is characterised by an austenitic structure with numerous growth twins of a mean grain size of $\bar{A}$ = 2120 μm^2 (Fig. 7). An increase of the initial soaking temperature to 1150°/2h results in an increase of the grain mean plane section area to the size of $\bar{A}$=6296 μm^2 (Fig. 8).

In the alloy substructure in its initial condition, a slight amount (ca. 0.3%) of undissolved precipitations and elevated dislocation density were evidenced (Fig. 9). Presence of titanium compounds, such as TiC carbide, TiN nitride, Ti(C,N) carbonitride, $Ti_4C_2S_2$ carbosulfide, Laves' Ni_2Si phase and boride MoB was disclosed in the phase composition of the undissolved precipitations [2]. The average dislocation density in the supersaturated material amounted to: $\rho = 4.88\times10^{12}$ m^{-2} (for the 1100°C/2h option) and $\rho = 3.99\times10^{12}$ m^{-2} (for the 1150°C/2h option).

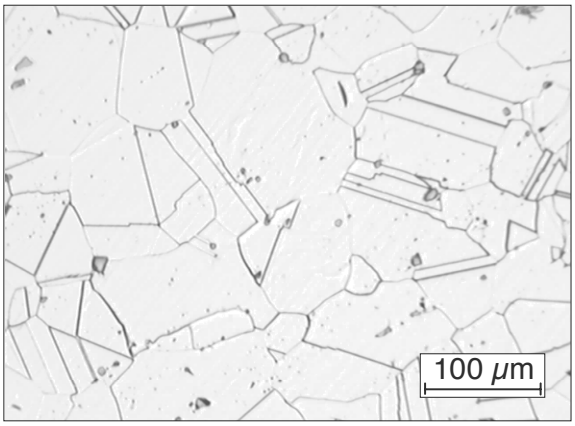

Fig. 7. Microstructure of alloy after pre-soaking 1100°C/2h. Grain size $\bar{A}$ = 2120 μm^2

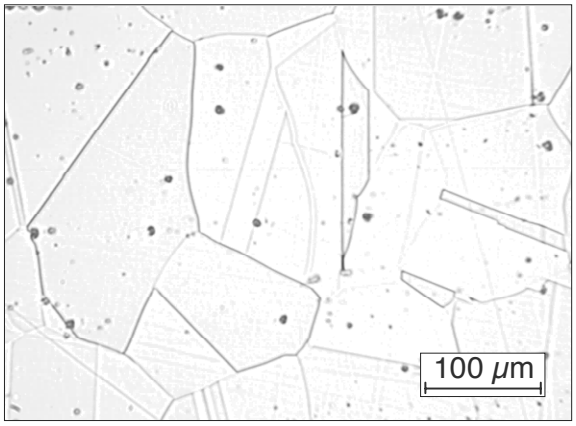

Fig. 8. Microstructure of alloy after pre-soaking 1150°C/2h. Grain size $\bar{A} = 6296\ \mu m^2$

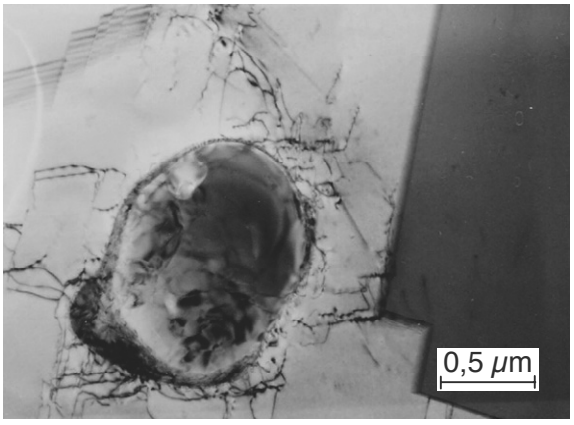

Fig. 9. Substructure of alloy in initial state after pre-soaking 1100°C/2h. The twinned austenite with an increased density of dislocations and undissolved particle of $Ti_4C_2S_2$

After the samples had been deformed at a temperature of 900°C and speed of 0.1 s^{-1}, advanced stages of dynamic recovery were evidenced in the alloy substructure. In areas characterised by high defectiveness of austenite, a cellular dislocation structure and subgrain structure is forming, of diversified dislocation density (Fig. 10). In the samples deformed at a temperature of 950°C and speed of $1.0s^{-1}$, nuclei of recrystallized grain in in the subgrain matrix as well as recrystallized microareas were found. The initiated process of dynamic recrystallization is characteristic for both options of initial soaking applied in the experiment (Fig. 11).

The alloy deformed in the range of temperatures of 1000-1050°C shows properties characteristic of dynamically recrystallized structures. To a large extent, the austenitic structure is composed of recrystallized grain free of dislocation, whereas in the subgrain, one can notice an advancing process of further improvement of the substructure recovery (Fig. 12). At the highest deformation temperatures in the range of 1100-1150°C, a continuous process of the structure reconstruction, known as repolygonization, is observed. It consists in a repeated regrouping of dislocation together with the formation of new subboundaries of the subgrain and polygonal walls (Fig. 13).

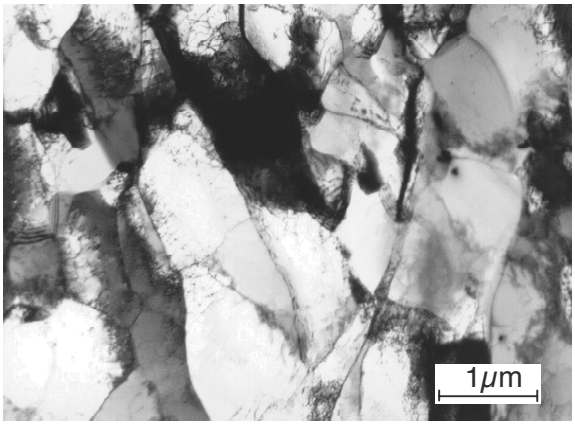

Fig. 10. Substructure of alloy after deformation at 900°C temperature with the rate 0.1 s^{-1}. Cellular dislocation substructure. Pre-soaking of the alloy: 1100°C/2h

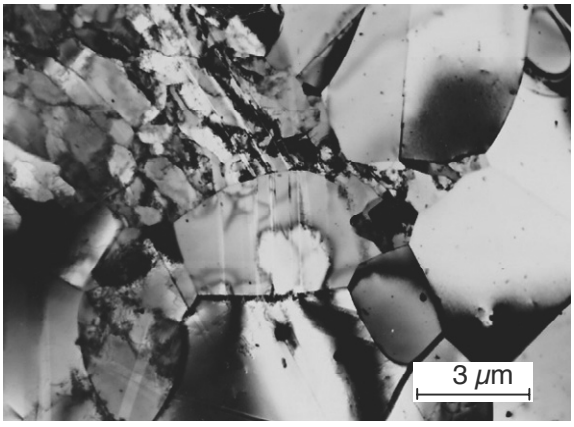

Fig. 11. Substructure of alloy after deformation at 950°C temperature with the rate: $1.0s^{-1}$.The recrystallized microareas of austenite. Pre-soaking of the alloy: 1100°C/2h

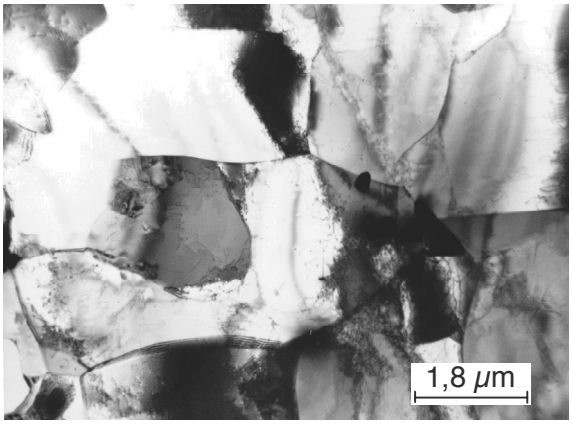

Fig. 12. Substructure of alloy after deformation at 1000°C temperature with the rate 0.1 s^{-1}. Nucleation of new recrystallized grain. Pre-soaking of the alloy: 1150°C/2h

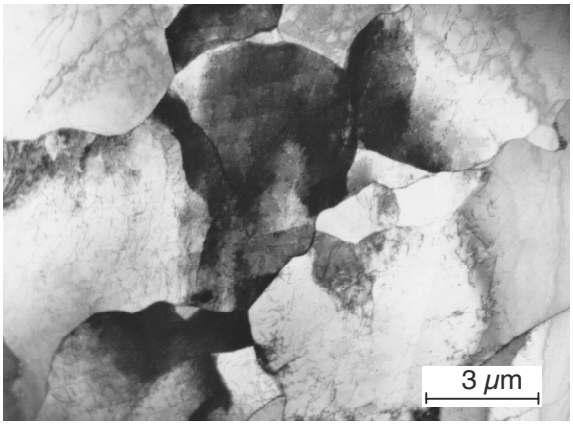

Fig. 13. Substructure of alloy after deformation at 1100°C temperature with the rate: 0,1 s^{-1}. Process of austenite repolygonization. Pre-soaking of the alloy: 1150°C/2h

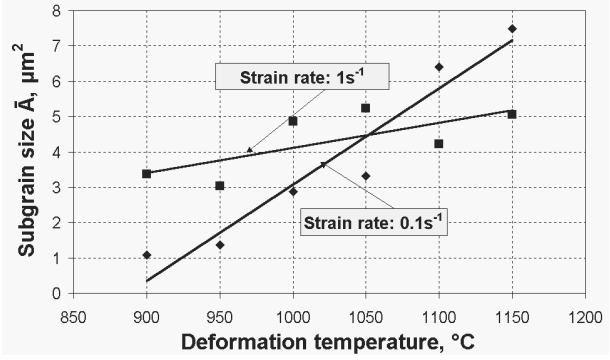

Fig. 14. Influence of temperature and strain rate on mean subgrain size. Pre-soaking of the alloy: 1100°C/2h

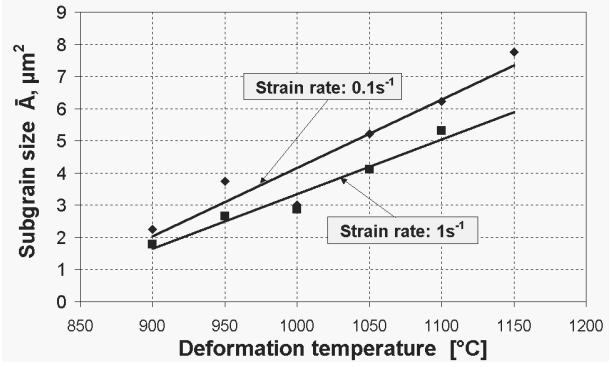

Fig. 15. Influence of temperature and strain rate on mean subgrain size. Pre-soaking of the alloy: 1150°C/2h

The course of changes in the subgrain size depending on the alloy deformation temperature and speed is shown in Figs. 14 and 15. It results from the presented dependencies that an increase of the deformation temperature is accompanied by an increase of the subgrain size. The average size of the subgrain was changing in the range from 1.0 to 7.8 μm^2. The influence of deformation speed on the subgrain size depends significantly on the alloy initial soaking temperature, i.e. the initial size of austenite grain.

The course of changes in the dislocation density depending on the deformation temperature and speed is presented in Figs. 16 and 17. As results from the presented dependencies, an increase in the deformation temperature is accompanied by a decrease of dislocation density. The values obtained for dislocation density change in the range of 0.8-2,5 $\times 10^{13}$ m^{-2}.

For both options of the alloy initial soaking, higher dislocation density values were obtained for a lower deformation speed, i.e. 0.1s^{-1}. This can be explained by a different mechanism of cyclic dynamic recrystallization occurring at small deformation speeds and consisting in multiple strengthening and recrystallization of the alloy structure.

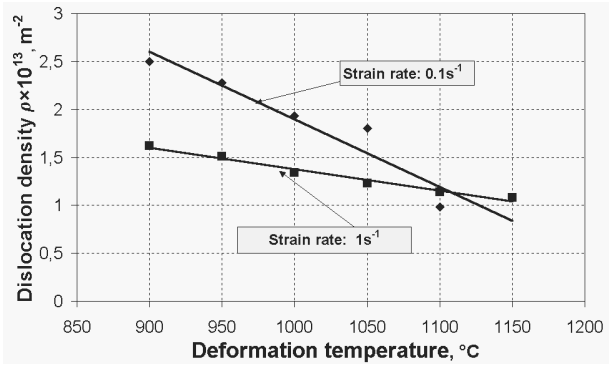

Fig. 16. Influence of temperature and strain rate on the mean dislocation density. Pre-soaking of the alloy: 1100°C/2h

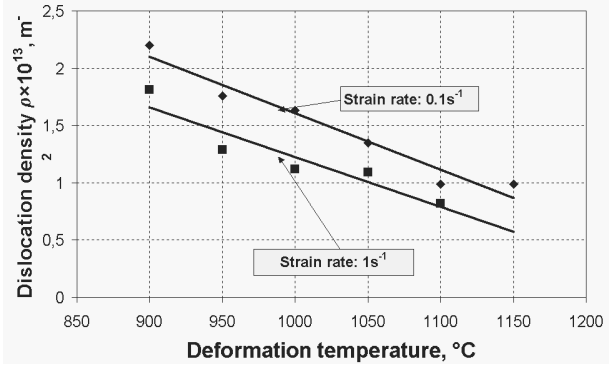

Fig. 17. Influence of temperature and strain rate on the mean dislocation density. Pre-soaking of the alloy: 1150°C/2h

5. Conclusions

On the basis of the investigations and analysis of the results, the following conclusions may be formulated:

1. Flow curves of the investigated Fe–Ni austenitic alloy have shapes characteristic of a material in which recovery and dynamic recrystallization processes take place.

Characteristics of the alloy plastic properties during hot deformation depend considerably on the initial soaking temperature and torsion parameters.

1. Optimum values of yield stresses and threshold deformation were obtained for the alloy after its initial soaking at 1100°C/2h and deformation speed of 0.1 s^{-1} in the temperature range of 1050-950°C. Application of higher soaking temperatures and deformation speeds is not recommended due to a growth of the austenite grain, difficulties in the course of the recover and recrystallization processes as well as a decrease of the alloy's plasticity.
2. For both options of initial soaking, a considerable influence of the alloy deformation parameters on the maximum yield stress was found. The dependence between the maximum yield stress (σ_{pp}) and the Zener-Hollomon's parameter has been described by means of a power function in the following form: $\sigma_{pp} = A \times Z^n$.
3. The alloy analysed is characterised by high activation energy of the plastic deformation process, whereas its value depends on the initial soaking conditions. For the alloy after initial soaking at 1100°C/2h, the activation energy estimated in the range of the deformation temperatures applied amounted to Q = 483 kJ/mol. In the case of the alloy deformation after initial soaking at 1150°C/2h, the activation energy was higher and amounted to Q = 563 kJ/mole.
4. The investigations into the influence of the hot deformation parameters on the substructure of the Fe–Ni austenitic alloy revealed the successive recovery, recrystallization and repolygonization processes. None of the analysed stages of changes in the substructure does not constitute an individual process.
5. An essential technological parameters influencing the subgrain size and dislocation density is the process temperature. The alloy deformed at temperatures of 900-950°C is characterised by higher dislocation density (ρ=1.5-2.5×$10^{13}$$m^{-2}$) and inhomogeneity of dislocation inside the subgrain whose area is considerably small, approximately 1÷3 μm^2.
6. An increase of the alloy deformation temperature to the range of 1000-1050°C results in the subgrain enlargement ($\bar{A}$=3-5μm^2) with a simultaneous drop of the dislocation density inside them. The mean values obtained for the dislocation density were in the range of 1.2-2.0×10^{13} m^{-2}.
7. At the highest temperatures of the alloy deformation, i.e. in the range of 1100-1150°C, a repolygonization process was observed in the samples. The process was accompanied by a further growth of subgrain up to 5-7.8 μm^2 as well as a drop of the average dislocation density to ca. 0.8÷1.1×10^{13} m^{-2}.
8. The influence of the alloy strain rate on the size of the subgrain and the dislocation density is a complex issue and depends on the initial value of austenite grain as well as on the mechanism of dynamic recrystallization.

Acknowledgements

This work was supported by the Committee of Scientific Research of Poland under grant No. 7 T08A 038 18.

References

[1] K.J. Ducki, M. Hetmańczyk, D. Kuc, The deformability and substructure of hot-deformed high-temperature Fe–Ni austenitic alloy, Proceedings of the 11th International Scientific Conference on the "Contemporary Achievements in Mechanics, Manufacturing and Materials Science" CAM3S, Gliwice-Zakopane, 2005, (CD-ROM).

[2] K.J. Ducki, Precipitation and growth of intermetallic phase in a high-temperature Fe–Ni alloy, Journal of Achievements in Materials and Manufacturing Engineering 18 (2006) 87-90.

[3] H. Gao, G.C. Barber, Q.A. Chen, High temperature deformation of a Fe-based law nickel alloy, Journal of Materials Processing Technology 142 (2003) 52-57.

[4] E. Hadasik, Methodology for determination of the technological plasticity characteristics by hot torsion test, Archives of Metallurgy and Materials 50 (2005) 729-746.

[5] H.S. Jeong, J.R. Cho, H.C. Park, Microstructure prediction of Nimonic 80A for large exhaust valve during hot closed dieforging, Journal of Materials Processing Technology 162-163 (2005) 504-511.

[6] H.J. Klaar, P. Schwaab, Ö. Werner, Round Robin investigation into the quantitative measurement od dislocation density in the electron microscope, Praktische Metallographie 29 (1992) 3-26.

[7] M. Kohno, T. Yamada, A. Susuki, S. Ohta, Heavy Disk of Heat Resistant Alloy for Gas Turbine, Proceedings of Internationale Schmiedetagung, Düsseldorf, 1981.

[8] M. Konter, M. Thumann, Materials and manufacturing of advanced industrial gas turbine components, Journal of Materials Processing Technology 117 (2001) 386-390.

[9] U. Martin, U. Mühle, H. Oettel, The quantitative measurement of dislocation density in the transmission electron microscope, Praktische Metallographie 32 (1995) 467-477.

[10] H.J. McQueen, S. Yue, N.D. Ryan, E. Fry, Hot working characteristics of steels in austenitic state, Journal of Materials Processing Technology 53 (1995) 293-310.

[11] N.K. Park, I.S. Kim, Y.S. Na, J.T. Yeom, Hot forging of a nickel-base superalloy, Journal of Materials Processing Technology 111 (2001) 98-102.

[12] I. Schindler, J. Boruta, Utilization potentialities of the torsion plastometer, department of metal forming, Silesian University of Technology, Katowice 1998.

[13] C.M. Sellars, Role of computer modelling in thermomechanical processing, Materials Engineering (1998) 100-107.

[14] J.M. Zhang, Z.Y. Gao, J.Y. Zhuang, Z.Y. Zhong, Grain growth model of IN718 during holding period after hot deformation, Journal of Materials Processing Technology 101 (2000) 25-30.

[15] L.X. Zhou, T.N. Baker, Effects of strain rate and temperature on deformation behaviour of IN 718 during high temperature deformation, Materials Science and Engineering A177 (1994) 1-9.

[16] M. Zhang, Z.Y. Gao, Z.Y. Zhuang, Z.Y. Zhong, Modeling of grain size in superalloy IN718 during hot deformation, Journal of Materials Processing Technology 88 (1999) 244-250.